

# Preliminary results of the OCTL to OICETS optical link experiment (OTOOLE)

<sup>a</sup> Keith E. Wilson\*, <sup>a</sup> Joseph Kovalik, <sup>a</sup> Abhijit Biswas,  
<sup>a</sup> Malcolm Wright, <sup>a</sup> William T. Roberts, <sup>b</sup> Yoshihisa Takayama, <sup>c</sup> Shiro Yamakawa

<sup>a</sup>NASA Jet Propulsion Laboratory,  
4800 Oak Grove Dr. Pasadena CA 91001-8099

<sup>b</sup>National Institute of Information and Communications Technology (NICT),  
4-2-1 Nukui-Kitamachi, Koganei, Tokyo 184-8795, Japan

<sup>c</sup>Japan Aerospace Exploration Agency (JAXA),  
2-1-1 Sengen, Tsukuba, Ibaraki 305-8505, Japan

## ABSTRACT

JPL in collaboration with JAXA and NICT demonstrated a 50Mb/s downlink and 2Mb/s uplink bi-directional link with the LEO OICETS satellite. The experiments were conducted in May and June over a variety of atmospheric conditions. Bit error rates of  $10^{-1}$  to less than  $10^{-6}$  were measured on the downlink. This paper describes the preparations, precursor experiments, and operations for the link. It also presents the analyzed downlink data results.

Keywords: Lasercom, Table Mountain, OICETS, OCTL, optical communications

## 1. INTRODUCTION

The Japan Aerospace Exploration Agency (JAXA) launched the Optical Inter-orbit Communications Engineering Test Satellite (OICETS) into a 610-km low Earth orbit (LEO) 97.8-degree inclination on August 23, 2005<sup>1</sup>. The OICETS performed an optical inter-satellite link with ESA's ARTEMIS geostationary satellite, and represented the second of the first series LEO-GEO optical links<sup>2</sup>; the first having been performed between the French SPOT-4 satellite and the European Space Agency's ARTEMIS<sup>3</sup>. Although OICETS was primarily designed for the inter-satellite optical communications experiments the satellite could also support a space-to-ground link<sup>4</sup>. This design feature extended both the utility and the useful life of the satellite.

The OICETS star trackers were mounted on the LUCE (Laser Utilizing Communications Experiment) side of the satellite. OICETS was inverted to point LUCE to the ground station to complete the optical communications link. Navigation of the inverted spacecraft during space-to-ground links was accomplished using the onboard gyros. JAXA scheduled drift rate estimation activities every fortnight to provide accurate satellite position information to ground stations.

The first set of bi-directional space-to-ground optical links with the OICETS was performed by NICT in September 2006 and the satellite was reactivated in October 2008 for a new space-to-ground optical link campaign<sup>4,5</sup>. In May 2009 JPL collaborated with JAXA and NICT to demonstrate the bi-directional optical communications link between OICETS and the Optical Communications Telescope Laboratory (OCTL).

The OCTL is shown in Figure 1 and was the ground station for the OTOOLE demonstration. At 34-degrees latitude and located at 2.2-km altitude in Wrightwood CA the facility affords access to satellites in a variety of inclinations. The facility houses a 1-m El/Az mount, f#75.8 coudé focus instrument with a co-aligned 20-cm f#7.5 acquisition telescope.

\* [kwilson@jpl.nasa.gov](mailto:kwilson@jpl.nasa.gov); phone 818 354-9387; fax 818 393-6142.



Figure 1. The OCTL telescope at the JPL Table Mountain Facility.

OTOOLE link opportunities were scheduled twice per week beginning May 21 and ending June 11. The experiment objectives were to:

1. Demonstrate acquisition and tracking of low (600km 98 degree inclination) LEO satellite from OCTL
  - a. Bi-directional optical communications with OICETS LEO satellite from the OCTL
    - i. 2Mbps uplink
    - ii. 50 Mbps downlink
2. Test operational issues involved with high-bandwidth LEO satellite optical communications support
  - a. Validate optical communications link models including fade statistics
  - b. Validate aperture averaging effect on downlink
3. Characterize link performance under a variety of atmospheric and background conditions e.g.
  - a. Partial cloud cover & moonlit sky

## 2. OTOOLE OPERATIONS PLANNING

OTOOLE operations planning at JPL began in January 2009. An interagency Letter of Agreement (LOA) between JAXA and NASA resulted in a May 21, 2009 authorized OTOOLE start date. Procedures to conduct the satellite-ground demonstration began at JAXA/NICT six weeks before the scheduled experiment date. The ground facilities plan to control OICETS was drafted from the long-term prediction of the satellite visibility windows. The windows for OCTL were computed simultaneously taking into consideration restrictions, such as the sun direction from LUCE, and the OCTL 20 degree tree line. Final modifications to the visibility windows of the ground facilities were recalculated two weeks before the experiment from the latest tracking information.

The updated calculations allowed a more accurate estimate and a detailed schedule of the availability of each ground facility to access the satellite and upload commands and verify the satellite status to be prepared. In the event that the calculations showed that there were more than two opportunities to conduct the experiment, the candidate windows were presented to the OCTL team for selection. One week prior to the planned experiment, the access times were reconfirmed based on the most recent orbit information.

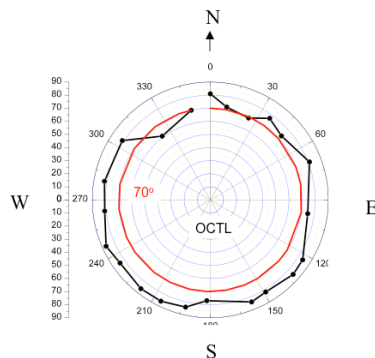


Figure 2. The OCTL tree line

Typically twenty-four hours before the experiment JAXA and NICT provided the most recent satellite ephemeris and the exact experiment times. According to the satellite operation scenario for OTOOLE JAXA generated and uplinked to the OICETS the appropriate commands and parameters to control LUCE. Post-experiment telemetry was downloaded from OICETS to the scheduled ground facility and forwarded to NICT for quick-look analysis. These procedures were repeated for every trial through the campaign.

Seven passes were identified occurring on Tuesdays and Thursdays during the allocated OTOOLE demonstration period. Of the allocated opportunities, one pass conflicted with a JAXA drift rate estimation operation, and two of the passes culminated at an elevation just above the OCTL tree line shown in Figure 2. The remaining four experiments were performed successfully under a variety of weather conditions.

Outdoor laser beam propagation from the OCTL is under the purview of the Federal Aviation Administration (FAA) and the US Space Command Laser Clearinghouse. OCTL's three-tiered laser safety system is a facility asset that is integrated to its outdoor laser beam propagation projects<sup>6</sup>. The NOHD defines the range beyond which laser is eye safe. The nominal ocular hazard distances (NOHD) for the beacon and communications lasers were 174-m and 24-m, respectively. The Laser Clearinghouse was apprised of the OTOOLE experiment times and waived the OTOOLE lasers from predictive avoidance coordination. This waiver however did not extend to the precursor experiments that used high power lasers and narrow optical beams. During both the precursor experiments and the OTOOLE demonstration outside observers were posted to alert operators to aircraft at risk.

### 3. PRECURSOR EXPERIMENTS

The OICETS interface control document (ICD) detailed downlink modulation format, wavelength, beam divergences transmitted power<sup>7</sup>. It also detailed the required uplink beacon wavelength and irradiance and communications laser's modulation format, data rates and wavelengths. In addition the ICD specified that the accuracy of the knowledge of the satellite's position was 1 km at 1000 km.

To prepare for the OTOOLE demonstration, the OCTL team performed a series of precursor experiments with LEO retro-reflecting satellites to validate the telescope's ability to point and track LEO satellites from the consolidated predict file format (CPF). Per the TAA, JAXA provided OICETS ephemeris to OCTL in the CPF format. Telescope pointing and tracking precursor experiments were also performed as a routine task preceding each OTOOLE track.



Figure 3. High power 532-nm OTOOLE precursor experiments laser uplinked through the 1-m OCTL telescope.

Figure 3 shows the frequency-doubled 532-nm Nd:YAG laser coupled to the 1-m OCTL telescope. The 10-ns, 10-Hz, Q-switched laser output 0.5J/pulse and was transmitted in two equal power beams of 30-uradian divergence to targeted Stella (800-km), Starlette (812-km), and Ajisai (1490-km) retro-reflecting LEO satellites<sup>8</sup>. A solid-state photomultiplier tube at the focus of the 1-m telescope detected the retro-reflected signal. The optical train is shown in Figure 4 and has been discussed in more detail in reference 9. The uplink intensity variance was reduced a factor of two by separating the laser beam into two equal power beams propagated on either side of the 1-m telescope. Multi-beam uplinks are an established uplink scintillation mitigation strategy<sup>10</sup>.

Figure 5 shows the retro-reflected signal from two of the target satellites. These experiments confirmed the telescope’s ability to track LEO targets to within the 30-urad beam width; a pointing accuracy better than that required to point the 1-mrad OTOOLE uplink communications beam. The gaps in the returns are due to cloud patches and the Laser Clearinghouse predictive avoidance uplink transmission interrupts.

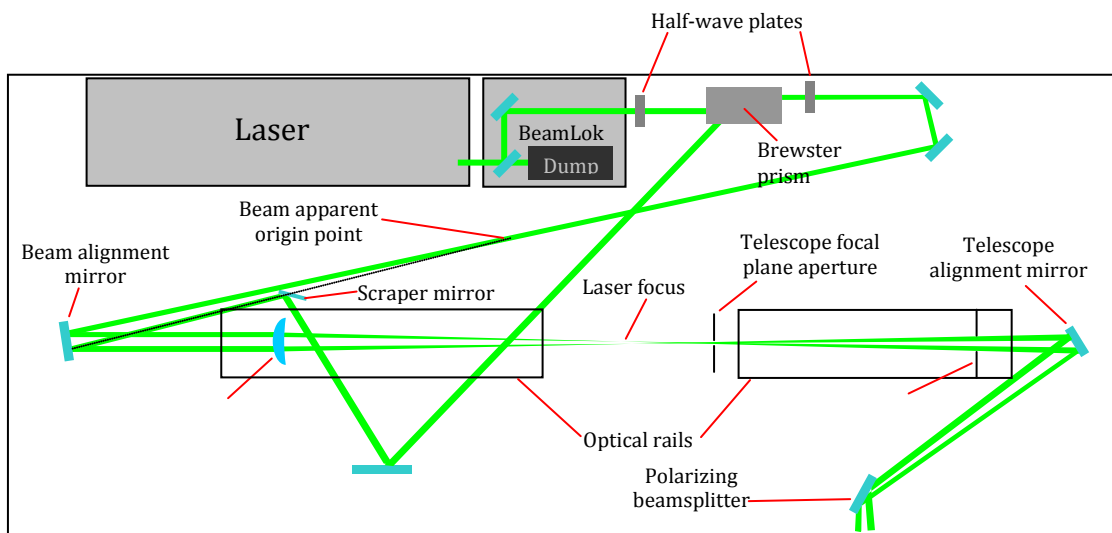


Figure 4. Layout of laser beam generation and alignment system for precursor experiments.

Early laboratory tests were conducted to validate and optimize the receiver performance at the 50 Mb/s downlink data rate, and the output of the uplink beacon and of the 2 Mb/s data rate communication laser. Both uplink and downlink data formats were a PN-15 Pseudo Random Bit Stream (PRBS). The uplink format was binary pulse position modulation (BPPM) and the downlink was On-Of-Key (OOK). The BPPM uplink format was generated by a simple logic circuit modifying an OOK data stream<sup>11</sup>. Analysis predicted downlink signal strengths of 100’s nW to 1  $\mu$ W. Laboratory tests of the receiver detector showed that the clock and data recovery unit could lock with a BER of  $10^{-6}$  at an input power level of 34nW, 50Mb/s data rate.

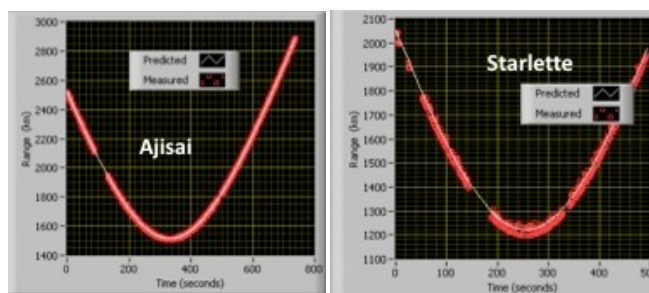


Figure 5. Retro-reflected signal returns from tracked 1500-km altitude Ajisai and 800-km altitude LEO satellites.

#### 4. HARDWARE INTEGRATION AND TEST

##### 4.1 Downlink Receiver

Figure 6 is a schematic of the receiver platform. The platform was mounted to the 20-cm acquisition telescope that is co-aligned with the 1-m telescope. The first beam splitter transmitted 20% of the 847-nm downlink signal to the acquisition camera and visually confirmed the downlink. The remaining 80% of the received signal was transmitted through a 10-nm band pass filter centered at 850 nm to suppress the Rayleigh backscatter from the 801-nm and 819-nm uplink beams. The signal transmitted through the filter was equally split between a 600- $\mu$ m multimode fiber and a 1.5-mm diameter, 100-

MHz Si APD detector module. The other end of the fiber was coupled to the 25-KHz bandwidth silicon photodiode detector to measure the power fluctuations in the downlink. The APD measured the 49.3724-Mb/s On-Off-Key (OOK) downlink data stream for bit error rate (BER) analysis.

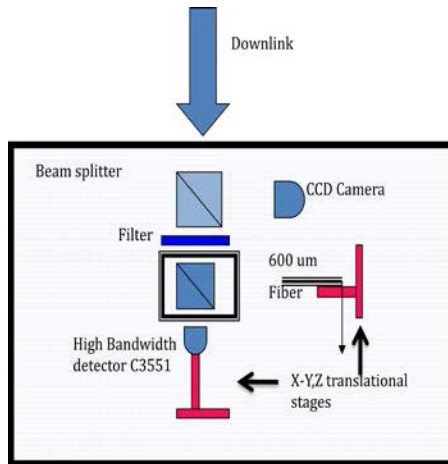


Figure 6. Schematic of the OTOOLE receiver showing the 100MHz bandwidth detector for the 50Mb/s downlink signal recovery for BER analysis and the 600-um core fiber that was coupled to the 5 KHz bandwidth photodiode detector to monitor the downlink intensity fluctuations.

The receiver platform integrated to the 20-cm telescope is shown in Figure 7. The low cutoff frequency (4KHz) of the avalanche photodiode detector precluded using a star for far-field alignment with the fiber-coupled detector a combination of techniques was used to align the receiver components on the optical platform to the 20-cm receiver telescope aperture. A bright star was used to align the fiber with the camera, and a 50Mb/s modulated transmitter source positioned 2-km away from the receiver was used to align the APD and fiber by maximizing the power received from the transmitter.

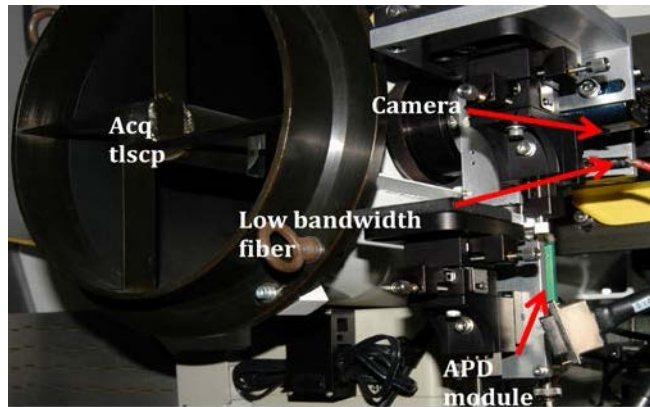


Figure 7. OTOOLE 20-cm receiver telescope with CCD camera, optical fiber to measure low-bandwidth downlink power fluctuations, and 100MHz bandwidth APD module for BER measurement.

#### 4.2 Uplink transmitter

Four 1-watt CW 801-nm lasers served as the coarse track uplink beacon. Three communications lasers uplinked the 2.048-Mb/s binary pulse position modulated (BPPM) pseudo-random bit stream, and also served as the source for fine tracking. High-power, single-mode lasers operating at 819 nm were not readily available, and the OTOOLE baseline design used two fiber Bragg grating 25-mW lasers temperature controlled at 55.5°C to operate at 819 nm and a 10-mW laser to generate the required uplink power.

Figure 8 is a schematic of the uplink. Figure 9 is a picture of the assembled and integrated components. The communications lasers were transmitted through a Raman filter and the beacon lasers were reflected from the filter to a 46-cm focal length off-axis parabola field mirror. The beacon and communications laser beams were expanded to 15-cm 7.5 cm respectively, and centered on the field mirror and coupled into the 1-m telescope. The beam sizes on the mirror determined the 2-mrad and 1-mrad divergences of the beams exiting the 1-m telescope.

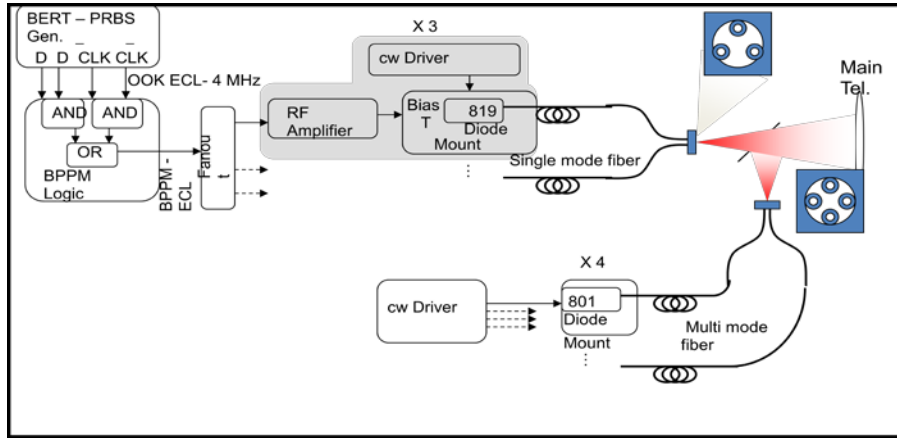


Figure 8. Schematic of OTOOLE transmitter optical train showing the beacon and communications lasers coupled to the off-axis parabola and onto 1-m telescope.

A multi-beam strategy was used in OTOOLE to mitigate uplink scintillation. The uplink beams were separated on the primary telescope mirror by distances greater than the Fried coherence length. The need for uplink scintillation mitigation was first demonstrated in the 1992 Galileo Optical Experiment, and its effect first demonstrated in the 1995 Ground-to-orbiter Lasercomm Demonstration<sup>12, 13</sup>. A more detailed description of the transmitter and receiver optical designs is given in reference 14.

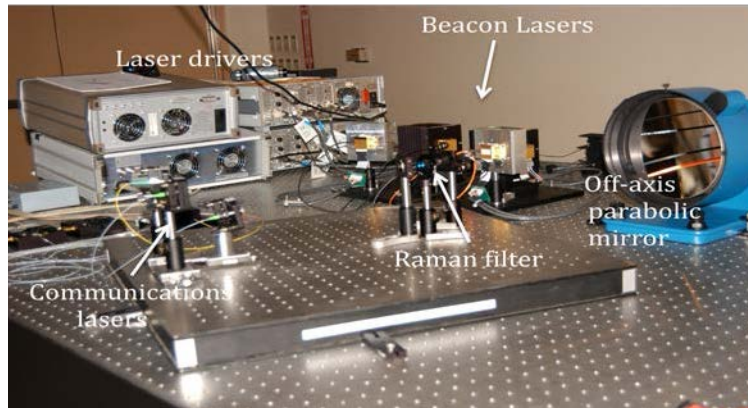


Figure 9. Picture of assembled OTOOLE uplink optical train.

### 4.3 Data Acquisition

The data acquisition system was designed to recover the satellite downlink signal from the APD, and the photodiode, and to monitor the output powers of the uplink beacon and communications lasers and the communications laser modulation. The system was software controlled and the data marked with GPS time stamp. Figure 10 is a block diagram of the system. Images of the downlink from the tracking camera were recorded on a high definition digital video recorder.

### Uplink

The beacon and data power levels were sampled at 25 MHz by a PCI based DAQ card. The beacon power was averaged and stored at 2 Hz. The depth of modulation of the communications lasers was averaged and stored at a 2 Hz.

## Downlink

The downlink data from the APD was split between the clock and data recovery chip and the PCI based digitizer. The clock and data outputs were sent to a BERT receiver. The average bit error rate was measured over a 0.5 second interval and transferred to the data computer over a GPIB interface. The other half of the APD signal was recorded directly by PCI based digitizer at 500 MHz. The digitizer retrieved 4000 samples of data at 2Hz and stored it on the data computer. The output from the low bandwidth detector was sent to a USB based DAQ that sampled continuously at a 5 kHz rate. The data were buffered and streamed to disk. The power level was also averaged over a 0.5 second interval and stored.

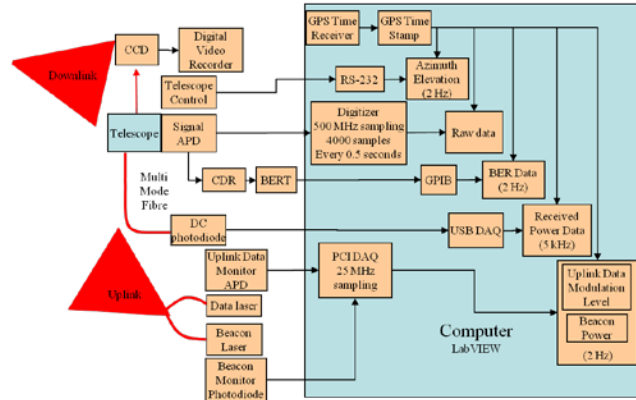


Figure 10. Block diagram of the data acquisition architecture.

## 5. OPERATIONS

Precursor experiments to retro-reflecting satellites were a part of the standard OTOOLE operation procedure before each OICETS pass and the Laser Clearinghouse predictive avoidances for the targeted satellites were retrieved and loaded into the OCTL laser safety system. The output power and alignment of the OTOOLE uplink lasers were checked after the precursor experiments and before the OTOOLE uplink. The telescope was pointed to a bright star for the final alignment check of the S1336 detector.

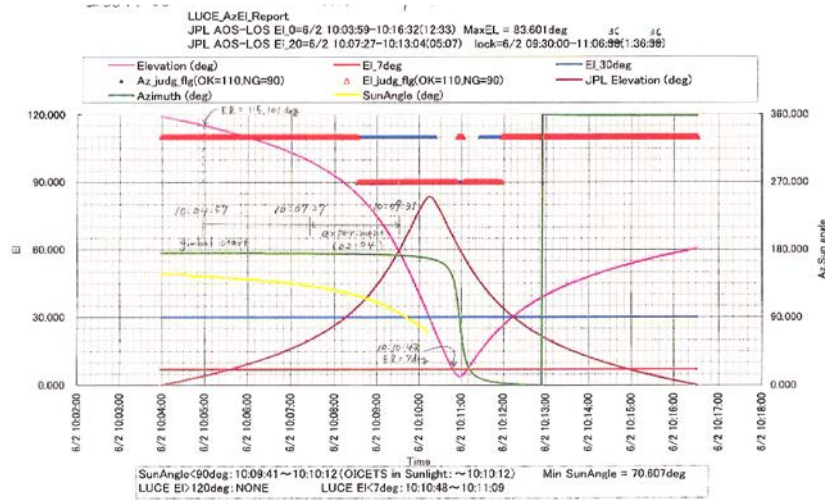


Figure 11. June 2 detail of OICETS track above the OCTL shows the experiment time and duration. The experiment began when the satellite entered the Earth shadow and ended as the satellite's elevation dropped below the OCTL tree line.

The OICETS passes from horizon to horizon lasted typically for approximately twelve minutes, with the OTOOLE links lasting for approximately two minutes, constrained either by the 20 degree OCTL tree line or by the sun-angle as seen by LUCE. LUCE's operation was strongly affected by Earthshine and by scatter off its optics when its optical axis was less

than 90-degrees to the sun OTOOLE was therefore scheduled for early morning passes against the dark Earth background.

Figure 11 shows the detail of the link opportunity for the June 2 pass. These graphics were sent by NICT to the OCTL team twenty-four hours before each pass. The figure shows the track starting at 20 degrees elevation and ending at 60 degrees elevation when the sun angle to LUCE's optical axis drops below 90 degrees. The link lasted for 124 seconds. Figure 12 captures the sequence of events from the initial acquisition of the sun-illuminated satellite to the detected downlink for the June 4 pass. Here there are approximately six minutes between the initial acquisition of the sunlit satellite and the onset of the downlink.

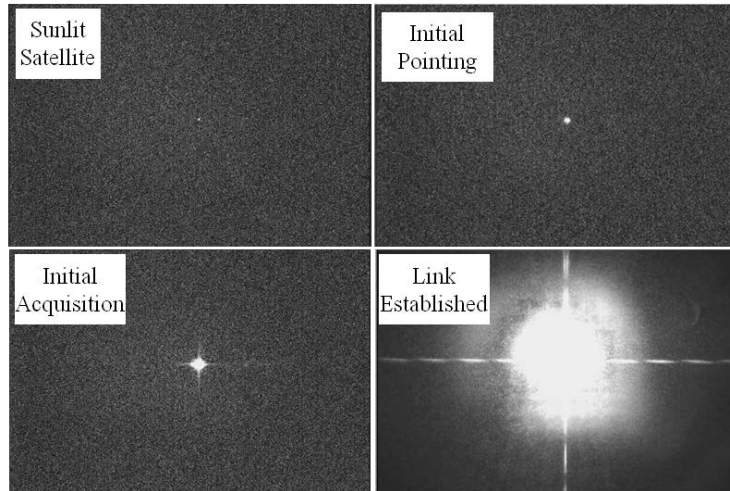


Figure 12. Shows the progression of the tracking for OTOOLE starting at the sunlit satellite to the downlink reception.

Table 1. OTOOLE journal for the four experiment days

<b>Experiment date</b>	<b>5/21/09</b>	<b>6/2/09</b>	<b>6/4/09</b>	<b>6/11/09</b>
Latest CPF files received, day, PST	5/20, 04:53	6/1, 04:52	6/3/2009, 04:52	6/10/09, 04:52
Start pass (0deg elev.)	2:53:00	3:04:00	03:22:30	3:46:50
End Pass (0 deg elev.)	3:05:00	3:16:30	3:43:10	3:59:20
Max elevation, deg	61	81	58	51
LUCE start (el, PST)	19.8 deg, 2:56:25	20 deg, 03.:07:27	53 deg, 03:28:25	20 deg, 02:52:04
LUCE end (el, PST)	54.2 deg, 3:01:49	60 deg, 03:09:31	20 deg, 03:30:43	48.7 deg, 02:54:19
Pass duration above tree line, sec	324	350	330	320
LUCE track duration, sec	324	124	138	135
OCTL link duration, sec	140	100	138	130
Link percentage of track	43.21%	80.65%	100.00%	96.30%
Weather	Clear	Clear	Overcast	Clear
Wind speed, km/hr	10.85 gusts to 29	10 gusts to 18	23 gusts to 40	6 gusts to 10
<b>Data products</b>				
Uplink beacon power, W	1.8	1.8	1.8	1.8
Average uplink comm power, mW	7	10	22	22
Downlink power received, nW	213-1075	170-300	150-300	100-750
Downlink comm BER	10E-1 => <10E-6	10E-2 => 10E-5	10E-4 => <10E-6	10E-1 => 10E-5

Table 1 is a journal entry from the four experiment opportunities. The data shows that the link was established and maintained under atmospheric conditions ranging from benign -low winds and clear skies of June 11- to severe -overcast

with sustained winds of 23 km/hr with gusts up to 40 km/hr. The downlink BER ranged from  $\sim 10^{-1}$  to less than  $10^{-6}$  with the lowest BERs observed on June 4, under the most severe atmospheric conditions.

During the June experiments the link was maintained for more than 80% of the track time. On the first opportunity, May 21, the downlink was observed for 43% of the scheduled track and was lost after the satellite reached culmination. For this track, the OCTL uplink was interrupted for several seconds as the satellite neared culmination, as the telescope was obscured by the dome as it unwrapped itself to track the satellite. The downlink losses of June 2, and June 11 were due to dropouts from LUCE pointing errors. Designed to perform inter-orbit laser communications with ARTEMIS, the angular velocity required for LUCE to maintain its pointing the ground station was much greater than that required for the inter-satellite link, and too fast for LUCE to track the ground station smoothly. This resulted increased pointing errors and dropouts in the downlink signal.

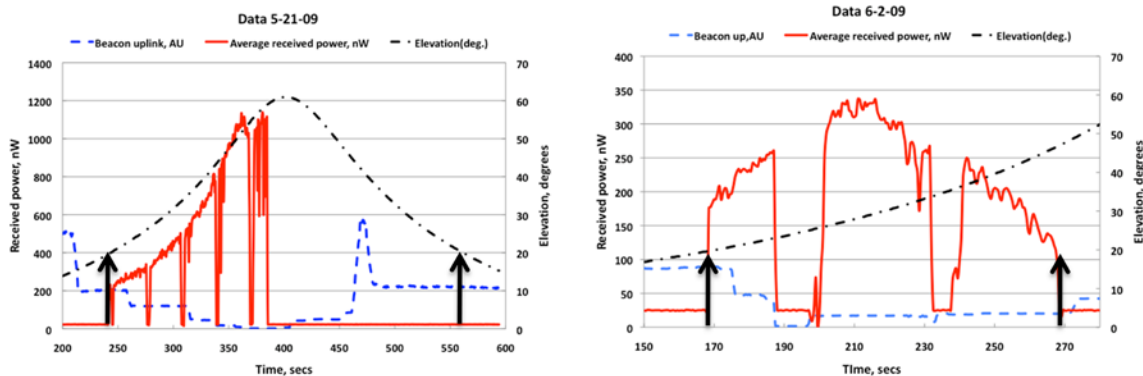


Figure 13. OCTL beacon uplink, OICETS downlink, and satellite elevation recorded during the pass. The arrows define the scheduled link duration.

In the June 4 and June 11 experiments, the beacon beam was turned off less than thirty seconds after the downlink was detected, leaving only the uplink communications beam for fine tracking. Figure 14 shows that the link was maintained for the duration of the scheduled experiments. The June 11 data show the characteristic dropouts. However, this was not seen in the June 4 data although the data does show three distinct deep fades during the pass.

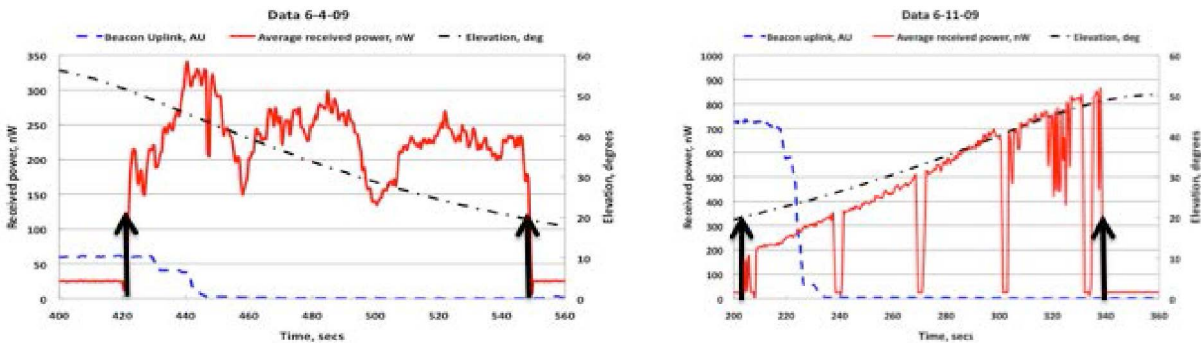


Figure 14. OCTL beacon uplink, OICETS downlink, and satellite elevation recorded during the pass. The arrows define the scheduled link duration. The beacon beam was turned off approximately 30 seconds after the downlink was detected. OICETS used a portion of the uplink communications beam for fine tracking and to maintain the downlink to the OCTL.

At the start of the pass both the beacon and communication beams were transmitted to the satellite, simultaneously. Figure 13 shows the measured downlink power the uplink beacon power in arbitrary units, and the satellite elevation during the May 21 and June 2 passes. On May 21, we observed a strong increase in downlink power with elevation reaching a maximum of greater than  $1\mu\text{Watt}$  near culmination, when the downlink was interrupted. The chart also shows that the beacon power was increased after the interruption and that the signal was not recovered before the end of the

pass. In the June 2 experiment the uplink beacon was attenuated to avoid saturating the coarse track sensor. Again the beacon was attenuated after the link was established. The June 2 link was maintained for the duration of the pass. As stated previously, the dropouts and downlink power fluctuations were due to LUCE pointing errors. The link was terminated at 50 degrees elevation on June 2, when the sun angle to the LUCE optical axis dropped below 90 degrees.

Downlink BER data ranged from 0.5 to  $10^{-8}$  and are shown in Figures 15 and 16 for the four experiment days. The data in general show low bit error rates  $\sim 10^{-8}$  when there are no dropouts. June 4 data show a BER of  $10^{-8}$  at received powers of 300-nW degrading to  $10^{-5}$  at the end of the pass as the satellite dropped in elevation and the received power dropped by 30%. The June 11 data show a marked correlation between the dropouts and the BER.

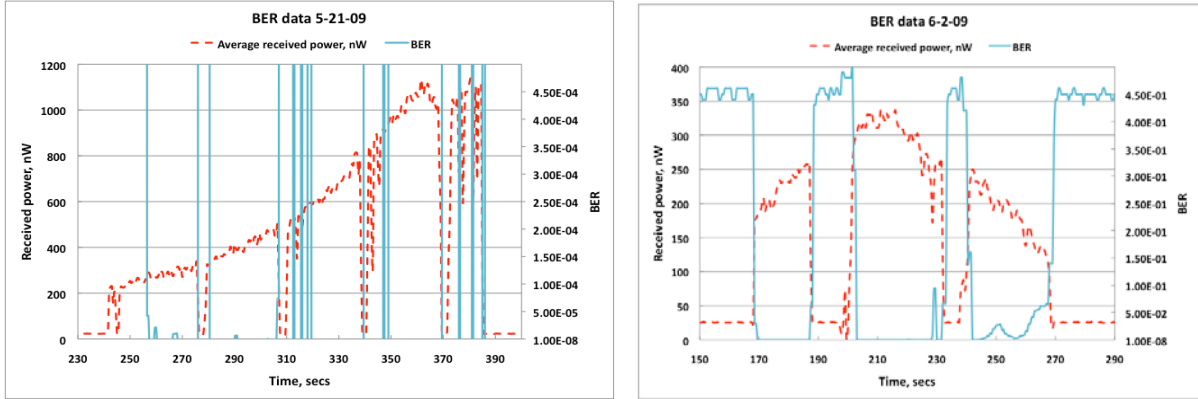


Figure 15. Bit error rate and downlink power measurements for May 21 and June 2.

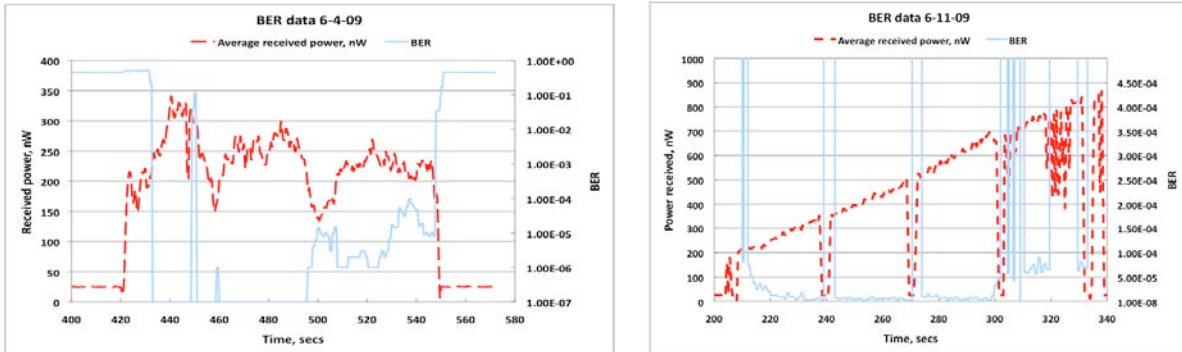


Figure 16. Bit error rate and downlink power measurements for June 4 and June 11.

## 6. DATA ANALYSIS

The recorded OICETS downlink data was compared to the analysis from our link models. The downlink power received from OICETS was predicted using equation (1) the standard link equation.

$$P_r = EIRP \times L_s \times \eta_{atm} \times G_R \times \eta_R \quad (1)$$

Where the EIRP represents the emitted isotropic radiated power,  $L_s$  is the space loss,  $\eta_{atm}$  is the atmospheric attenuation loss,  $G_R$  is the receiver gain and  $\eta_R$  is the receiver efficiency. The variation in  $L_s$  and  $\eta_{atm}$  were accounted for in predicting the received downlink power. The atmospheric attenuation loss was calculated from MODTRAN software where aerosol models corresponding to rural 23 km visibility and desert extinction were used for the desert extinction, the measured ground wind speed of 10 km/hr (3m/s) was used in the analysis.<sup>15</sup>

Figure 16 shows a comparison between the predicted and received laser power averaged for 500 milliseconds. The comparison shows that the atmospheric aerosol models chosen serve as good bounds for the prevailing conditions at the receiving station on June 11, 2009. Similar agreement (not shown) was also obtained on other passes.

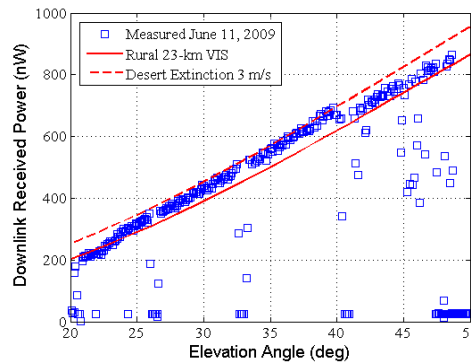


Figure 16. Comparison of measured and predicted downlink received power.

The scintillation index (SI) was calculated as a function of elevation angle from the measured data by choosing short (approximately 4-seconds) time windows. The histogram of the received signal power shows a reasonable, though imperfect agreement with a lognormal distribution. An example for one of the time windows is shown in Figure 17. Figure 18 shows the measured variation of the normalized variance or scintillation index with satellite elevation angle along with the modeled SI. The data show the expected reduction in SI with increasing elevation and are a good fit to the model when the aperture averaging of the 20-cm aperture is included in the analysis. A more detailed description of the analysis is given in reference 11.

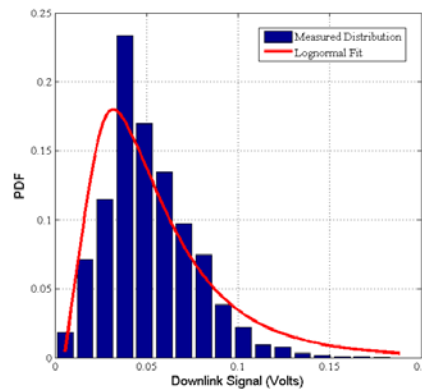


Figure 17. Comparison of the received downlink power histogram to a lognormal distribution

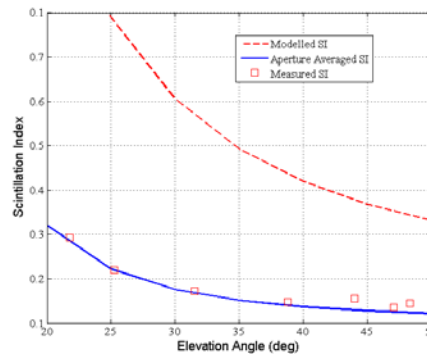


Figure 18. Measured SI variation with elevation angle measured on June 11, 2009, compared with the aperture averaged SI. The SI without aperture averaging is also shown for comparison.

## 7. CONCLUSIONS

A fast-paced project with a funding start in January 2009 and first bi-directional link with OICETS four months later i.e., May 2009, OTOOLE confirmed the readiness of the OCTL telescope to support future space-to-ground optical communications demonstrations.

OTOOLE successfully met all of its objectives namely, it:

1. Demonstrated acquisition and tracking of low (600km 98 degree inclination) LEO satellite from OCTL
2. Tested operational issues involved with high-bandwidth LEO satellite optical communications support, and validated our link models.
3. Characterized the link performance under a variety of atmospheric and background conditions.

## 8. ACKNOWLEDGEMENTS

The authors would like to acknowledge the contributions of the Dr. Naoto Kadowaki, and Dr. Morio Toyoshima, from NICT for their assistance in getting the OTOOLE demonstration approved. We would like to acknowledge the support Dr. Dimitri Antsos, and Dr. Steven Townes, Gina Madden of JPL and Dr. John Rush Dr. Barry Geldzahler, Ms. Irene Bibyk, and Dr. J.D. Miller of NASA. Finally we would like to thank our colleagues, Vachik Garkanian for the mechanical engineering support, Deronda Mayes for her support of the precursor experiments and Carlos Esproles for electronics circuit design and fabrication.

The work described here was performed at the Jet Propulsion Laboratory (JPL), California Institute of Technology under contract with the National Aeronautics and Space Administration (NASA).

## 9. REFERENCES

1. [http://www.jaxa.jp/projects/sat/oicets/index\\_e.html](http://www.jaxa.jp/projects/sat/oicets/index_e.html)
2. Yuuichi Fujiwara, Masaaki Mokuno, Takashi Jono, Toshihiko Yamawaki, Katsuyoshi Arai, Morio Toyoshima, Hiroo Kunimori, Z. Sodnik, A. Bird and B. Demellenne, "Optical inter-orbit communications engineering test satellite (OICETS)", *Acta Astronautica*, Volume 61, Issues 1-6, June-August 2007, Pages 163-175
3. Toni Tolker-Nielsen and Gotthard Oppenhauser "In-orbit test result of an operational optical intersatellite link between ARTEMIS and SPOT4, SILEX" SPIE, Free-Space Laser Communication Technologies XIV Proceedings Vol. 4635, January 2002, San Jose, CA.
4. Morio Toyoshima, Takashi Takahashi, Kenji Suzuki, Shinichi Kimura, Kenichi Takizawa, Toshiaki Kuri, Werner Klaus, Masahiro Toyoda, Hiroo Kunimori, Takashi Jono, Yoshihisa Takayama, and Katsuyoshi Arai, "Laser beam propagation in ground-to-OICETS laser communication Experiments" SPIE Defense and Security Proceedings Vol. 6551 April 2007 Orlando, FL
5. Yoshihisa Takayama, Morio Toyoshima, Yozo Shoji, Yoshisada Koyama, Hiroo Kunimori, Minoru Sakaue, Shiro Yamakawa, Yoshiyuki Tashima, Nobuhiro Kura, "Expanded laser communications demonstrations with OICETS and ground stations", SPIE Free-Space Laser Communication Technologies Proceedings, Vol, 7587 January 2010, San Francisco, CA.
6. Keith E. Wilson, "Laser Uplink Safety for Future NASA High-bandwidth Spacecraft Communications", ILSC March, 2009 Reno, NV.
7. JAXA, Draft OICETS Optical Interface Document February 2006.
8. [http://ilrs.gsfc.nasa.gov/satellite\\_missions/list\\_of\\_satellites/star\\_general.html](http://ilrs.gsfc.nasa.gov/satellite_missions/list_of_satellites/star_general.html)
9. Keith E. Wilson, Joseph Kovalik, Abhijit Biswas, and William Roberts "Development Of Laser Beam Transmission Strategies For Future Ground-to-Space Optical Communications", SPIE Defense and Security Proceedings Vol. 6551 April 2007, Orlando, FL
10. Deep Space Optical Communications, A. John Wiley & Sons publisher 2006 pp. 510-512. H. Hemmati Editor.
11. Joseph M. Kovalik, Keith E. Wilson, Abhijit Biswas, Malcolm W. Wright, William T. Roberts, "Data products for the OCTL to OICETS optical link experiment" SPIE Free-Space Laser Communication Technologies Proceedings, Vol, 7587 January 2010, San Francisco, CA.

12. K. E. Wilson and J. R. Lesh, "GOPEX: A Laser Uplink to the Galileo Spacecraft on its Way to Jupiter," SPIE Free-Space Laser Communication Technologies Proceedings, Vol. 1866, pp. 138-147, January 1993.
13. K. E. Wilson, J. R. Lesh, K. Araki and Y. Arimoto, "Overview of the Ground-to-orbit Lasercom Demonstration", Invited Paper SPIE Free-Space Laser Communication Technologies Proceedings, Vol. 2990, February 1997, San Jose, CA.
14. W. Thomas Roberts, Malcolm W. Wright, Joseph M. Kovalik, Keith E. Wilson, "OTOOLE System Design" SPIE Free-Space Laser Communication Technologies Proceedings, Vol, 7587 January 2010, San Francisco, CA.
15. Alexander Berk, Gail P. Anderson, Lawrence S. Bernstein, Prabhat K. Acharya, H. Dothe, Michael W. Matthew, Steven M. Adler-Golden, James H. Chetwynd, Jr., Steven C. Richtsmeier, Brian Pukall, Clark L. Allred, Laila S. Jeong, and Michael L. Hoke, "MODTRAN4 radiative transfer modeling for atmospheric correction" SPIE Proceedings Vol. 3756, pp. 348-353, July 1999, Denver, CO.